Pergamon

Int. J. Heat Mass Transfer. Vol. 37, No. 10, pp. 1423–1432, 1994

0017-9310/94 $7.00+0.00

0017-9310(94)E0008-I

Nucleate boiling characteristics of R-114, distilled water (H_2O) and R-134a on plain and rib-roughened tube geometries

SHOU-SHING HSIEH† and PAO-TUNG HSU

Department of Mechanical Engineering, National Sun Yat-Sen University, Kaohsiung, Taiwan, 80424, R.O.C.

(*Received* 27 *August* 1993 *and in final form* 24 *November* 1993)

Abstract—Pool nucleate boiling characteristics of R-114, distilled water (H_2O) and R-134a on plain and rib-roughened tubes (rib pitch 39.4 mm, rib height 4 mm, rib width 15 mm, number of element 8, rib angle 30–90°) geometries were extensively studied. Boiling data for both increasing/decreasing heat flux modes as well as the influences of heat flux level on heat transfer coefficient were presented and discussed. Enhancement performance ratios were calculated and compared for three different refrigerants and different tube geometries. Furthermore, it is found that smooth tube data agreed quite well with those of previous results.

INTRODUCTION

IN RECENT years significant progress has been made in understanding nucleate boiling heat transfer on the shell side of tubular heat exchangers in order to design improved evaporators for the process and refrigeration industries.

Numerous enhanced surfaces have been developed for pool nucleate boiling [1], and hundreds of experiments have been reported. These surfaces reveal a common angular geometry, which basically provided a high density of reentrant cavities that can create stable nucleation sites with minimum wall superheat [2], and they have been made into commercial tubes, such as High Flux [3], ECR40 [4], Thermoexcel-E [5], and GEWA-T [6, 7], etc. Marto and Lepere [8] used 15.8 mm OD plain copper tube and three copper enhanced surfaces (High Flux surfaces, Hitachi Thermoexcel-E surface and Wieland GEWA-T surface), with Freon-113 and Fluorinert FC-72, to measure pool boiling heat transfer coefficients. Hahne *et al.* [9] studied pool boiling heat transfer of R-11 at single tube and twin arrangement using both experimental and numerical methods. Furthermore, Ayub and Bergles [10] examined the hysteresis effect of the boiling R-113 on GEWA-T surfaces. Kenning [11] studied the variation of temperature on the back of a thin heated stainless steel plate during pool nucleate boiling of water using thermochromic liquid crystal. Chyu and Fei [12] focused on the region near the contact line where the restricted geometry makes the thermal environment very different from the environment outside of the restricted region, and found the effect of restricted liquid circulation and vapor movement on the heat transfer performance. In Webb and Pais [13], data are presented for nucleate pool boiling on five different horizontal tube geometries using five refrigerants at two saturation temperatures. The refrigerants tested are R-11, R-12, R-22, R-123 and R-134a at saturation temperatures of 4.44 and 26.7°C. The tube geometries tested are a plain tube, a 1024 fins m^{-1} integral-fin tube, and three commercially used enhanced tube geometries (GEWA TX19, GEWA SE and Turbo-B).

From the foregoing discussions, it is apparent that the two-phase interactions that occur in enhanced tube geometries during boiling can be very complex and can change with heat flux level, fluid properties, enhanced tube configurations, etc. For example, Wanniarahachchi *et al.* [2], Marto and Lepere [8] and Webb and Pais [13] pointed out that the boiling mechanism in an enhanced tube is different from that which occurs in a plain tube used in the process industry. This is due to different nucleation sites that augment bubble formations and to a different space arrangement that restricts natural circulation effects. As a result, it is quite difficult to use information obtained in one type of enhanced geometry and fluid combination, and apply it to another situation. Instead, a complete range of experimental data is needed in the open literature that covers various fluids, enhanced tube geometries, heat fluxes, so that theoretical models can be formulated and appropriately evaluated. This is particularly important in the refrigeration industry

† To whom correspondence should be addressed.

NOMENCLATURE

A	heat transfer area $2\pi r_o L$ [cm^2]
H	rib height [mm]
d_1	outside diameter [mm]
d_2	base diameter (rib root diameter) [mm]
h	wall heat transfer coefficient [W m^{-2} K^{-1}]
h_{fg}	latent heat of vaporization [J kg^{-1}]
k	thermal conductivity [W m^{-1} K^{-1}]
L	length of test tube [mm]
M	nucleation parameter, defined by equation (4)
N	number of rib elements
p	rib pitch [mm]
Q	heat transfer rate [W]
q	wall heat flux [W m^{-2}]
T	temperature
V	voltage
W	rib width [mm].

Greek symbol

θ	rib angle [°]
ΔT	temperature difference between the wall and the vapor [K]
ρ_v	density of vapor [kg m^{-3}]
σ_l	surface tension of liquid [N m^{-1}].

Subscripts

avg	average
e	equivalent
i	inside diameter
o	outside diameter
sat	saturated
w	tube wall.

where new, alternative refrigerants and refrigerant–oil mixtures are being proposed. In addition, no information is available regarding the onset of nucleate boiling in this of type rib-roughened enhanced tube geometry, roughened surface hysteresis effects, and the influence of previous history upon the incipient boiling condition of which they are very important during startup of a refrigeration system and process plant.

The objective of this study is, therefore, to establish additional baseline nucleate boiling data of R-114, distilled water (H_2O), and R-134a, from plain and rib-roughened tube geometries that represent a section of a refrigerant evaporator. Emphasis is placed on the influence of rib angle in the configuration upon the incipient boiling point. The data obtained are expected to serve as reference data for comparison with other roughened geometries and other refrigerants.

EXPERIMENTAL APPARATUS AND TEST PROCEDURES

Saturated nucleate boiling data were taken on a plain tube and a rib-roughened tube. The geometry details of these tubes are given in Table 1. Boiling tests were performed at three saturation temperatures, 14.8°C (R-114), 99.9°C (H_2O) and 4.4°C (R-134a). Some selected properties of R-114, distilled water and R-134a are listed in Table 2 for comparison.

Table 1. The dimensions of test tubes

Test tube	Tube (No.)	d_1 (mm)	d_2 (mm)	Number of rib elements	p (mm)	w (mm)	H (mm)	θ	A (mm^2)
Smooth	1	27	—†	—	—	—	—	—	27 992
Rib	2	27	19	8	39.4	15	4	90°	24 526
Rib	3	27	19	8	39.4	15	4	60°	27 059
Rib	4	27	19	8	39.4	15	4	45°	29 221
Rib	5	27	19	8	39.4	15	4	30°	33 254

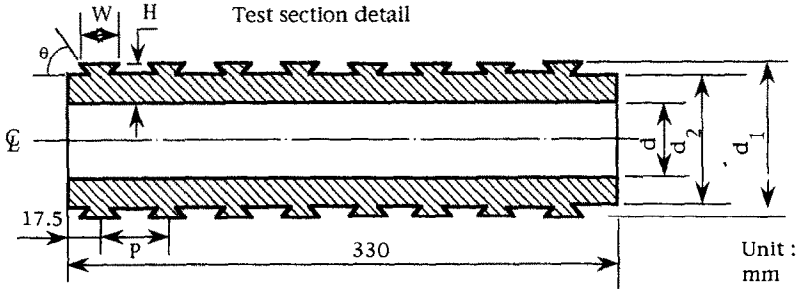

†'—' means data not available.

Table 2. Selected properties of refrigerants R-114, R-134a and distilled water

Property	R-114	R-134a	Distilled water
Chemical formula	$C_2Cl_2F_2$	CH_2FCF_3	H_2O
Molecular formula	170.94	102.03	18.0
Boiling point at 1 atm [°C]	3.85	−26.22	100.00
Freezing point [°C]	−93.9	−108	0.0
Critical temperature [°C]	145.65	101.0	374.14
Critical pressure [kgf cm^{-2}]	33.2	42.0	225.41
Density—saturated liquid [kg m^{-3}]	1440.8 (30°C)	1255 (25°C)	995.72 (30°C)
Density—saturated vapor [kg m^{-3}]	18.384 (30°C)	5.04 (25°C)	0.0304 (30°C)
Specific heat—saturated liquid [kJ kg^{-1} K^{-1}] (25°C)	0.159	0.3355	0.9983
Specific heat—vapor [kJ kg^{-1} K^{-1}]	0.162 (0°C)	0.2029 (25°C)	0.492 (113°C)
Latent heat vaporization [kJ kg^{-1}]	32.82 (0°C)	41.93 (bp)	535.79 (25°C)
Thermal conductivity—saturated vapor [W m^{-1} k^{-1}]	0.157	0.074 (20°C)	0.0246 (113°C)
Viscosity—saturated liquid [cp]	0.485 (0°C)	0.19 (30°C)	1.79 (0°C)
Viscosity—vapor [cp] (1 atm)	0.0115 (25°C)	0.0124 (30°C)	0.0127 (113°C)
Solubility of water [% w w^{-1}]	0.009 (25°C)	0.0773 (30°C)	100.00

The single-tube pool boiling apparatus consists of a rectangular boiling cell made of stainless steel and its entire loop is shown in Fig. 1(a). Figures 1(b) and (c) show the details of thermocouple positions and their measurements. The evaporator tube was designed to simulate a portion of a refrigerant-flooded evaporator (see Fig. 1(d) for detail). It was fabricated for a copper tube. The tube specimen is soldered to a flange at one side of the cell. The front and back sides of the cell consist of a tempered sight plexiglas to observe the boiling and to check the liquid level. The tank was insulated on all sides. Following Webb and Pais [13], each tube has two internal, axial machined grooves diametrically opposite and are used for thermocouple installation as shown in Fig. 2. The grooves are along the total tube length. The tube is soldered to a brass flange. The copper tubes were 27 mm in diameter over the ribs, with an inner diameter of 14 mm. Each cartridge heater 350 mm long and 13.95 mm in diameter with a maximum power output of 368 W is inserted in the copper tube. A sliding fit existed between the heater and the tube. Thermal contact between the heater and the tube is enhanced by applying a two-walled structure (MgO + quartz) of heat-sink compound on the heater before installing it in the tube. The DC power was supplied by a 100 V, 550 amp capacity DC rectifier. Two auxiliary heaters, each capable of 10 kW were mounted below the test tube to maintain liquid pool at saturated condition and to provide system pressure control. Power to the test section was controlled with a remote control box. For a given tube, the heat flux was calculated by dividing the electrical power (after it was corrected for small axial losses out each end of test tube) by the small tube surface area based upon an active heating length of 330 mm.

Vapor temperature was measured by a thermocouple (No. 5) near the top of the tube. Liquid temperatures were measured by two thermocouples (Nos. 3 and 4) located close to the free surface of the liquid. During operation, these two thermocouples were located in a frothy, two-phase mixture and were considered to be well representative of T_{sat} at the free surface. The average outer wall temperature of the instrumented test was obtained by averaging the two wall thermocouples (Nos. 1 and 2) in the copper grooves and correcting for the small radial temperature drop due to conduction across the copper wall. All copper–constantan thermocouples were made from the same roll of 0.152 mm diameter wire.

During all the tests, the saturation temperature was kept near 14.8°C (R-114), 99.9°C (water) and 4.4°C (R-134a), respectively. The liquid level was kept approximately 50 mm above the test tube. All the data were obtained and reduced with a computer-controlled data acquisition system. For each of these tests, an energy balance analysis was made for the test section. It was found that the energy balance was satisfied within 9.5%. The repeatability of the data was found good within ±7.8%.

Prior to filling with R-114/or distilled water and R-134a, the system was evacuated and leak checked. Once the system was felt to be vacuum tight, R114/or distilled water and R-134a was added to the cell by drawing it into the cell under vacuum. Before an experiment was started, the pool temperature was compared to the measured saturation pressure. A maximum power of 368 W was then supplied to the system, and boiling occurred for one hour before data were taken. The data were taken in order of increasing/decreasing heat fluxes. The power was increased (starting from 3 W) until the power limit (368 W) of the heater was reached so as to generate a good portion of the complete boiling curve. Finally, the power was reduced until nucleate boiling ceased. In measuring boiling heat transfer coefficients, great care must be exercised to ensure good accuracy. The following list shows those precautions.

1. The pool temperature was compared to the saturation temperature corresponding to the measured saturation pressure. This ensures that there are no noncondensibles in the system. It also verified that there is no subcooling in the liquid pool within ±0.2°C.

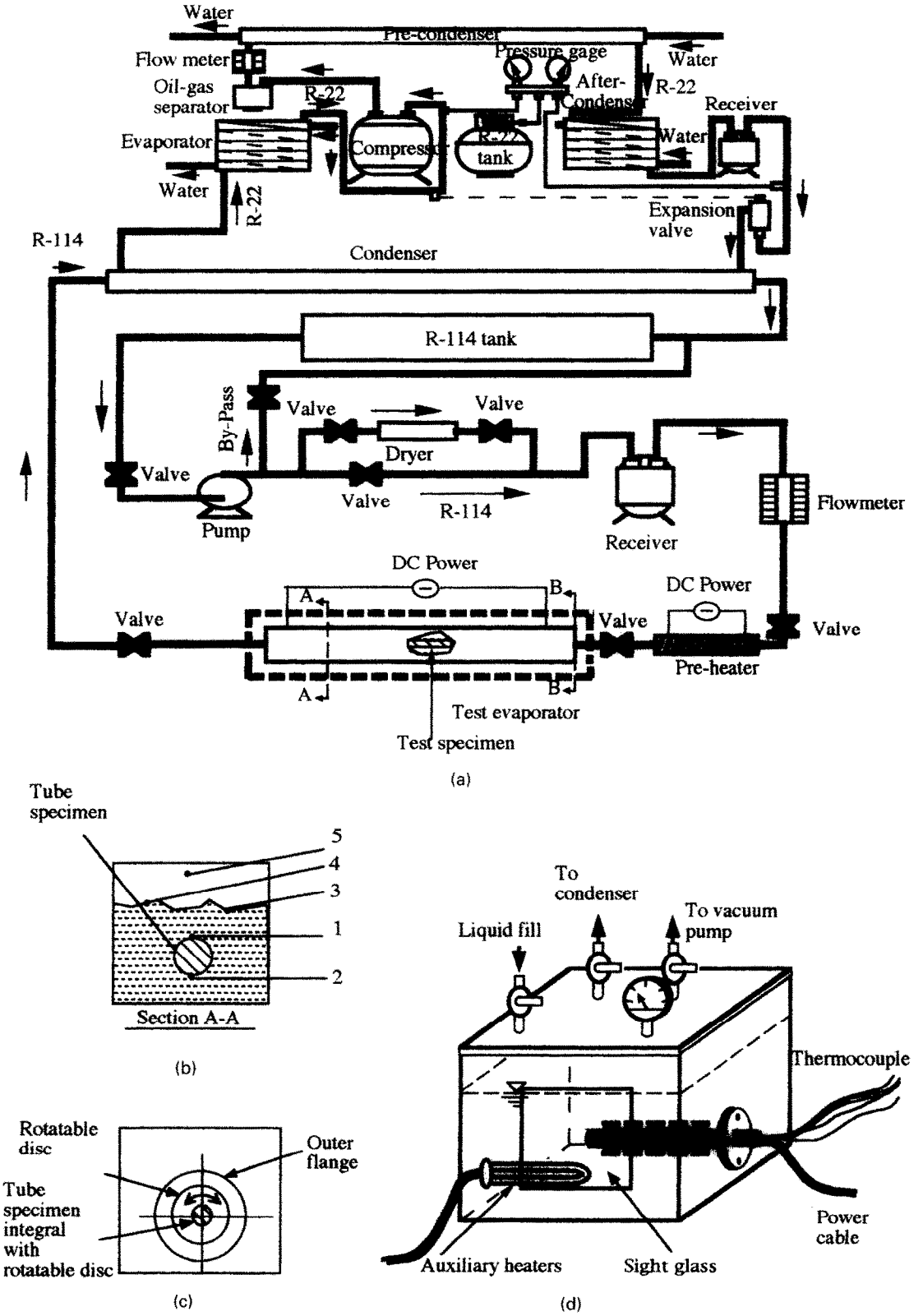

FIG. 1. (a) Entire loop of test facility. (b) Thermocouple location. (c) Section B-B. (d) Test evaporator details.

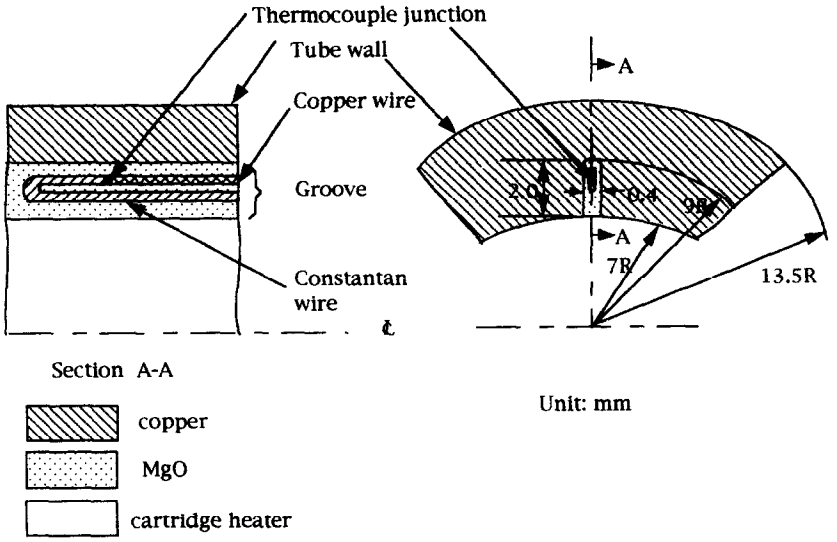

FIG. 2. Illustration of wall thermocouple installation.

2. The heater was tested for circumferential uniformity of heat flux. During this study, the instrumented test tubes were fabricated in similar way to those used by Hahne and Muller [14].

3. To smooth out any nonuniformities in heat flux caused by the cartridge heater, a copper sleeve with the aforementioned two-walled sink compound was used inside the test tube into which the cartridge heater was inserted with a tight mechanical fit. The outer diameter of the sleeve was machined to a diameter that was about 1.5 mm less than the inside diameter of the test tube. Its center was bored out to accommodate the cartridge heater.

4. To validate the thermocouple installation, the test tube was rotated, and the temperature was measured at different circumferential location by the two thermocouples (see Fig. 1(c) for detail).

The average wall temperature was used to define the heat transfer coefficient. It is defined as the average value of the thermocouple over six angular positions. The heat flux is based on the heated area of the tube which was contacted with liquid.

DATA REDUCTION

For each power input, the heat transfer coefficient was calculated on the basis of bulk fluid saturation temperature, tube heat flux and average of tube outside wall temperature. Because the temperature difference across the wall of the copper tube was large, the measured inside wall temperatures were corrected to give the outside tube wall temperatures

$$T_o = T_i - \frac{Q}{V}K[(r_o^2 - r_i^2)/4 - r_o^2/2\ln(r_o/r_i)]. \quad (1)$$

The average wall temperatures were defined as the average value of the two thermocouples over the six angular positions (both wall thermocouples at angular locations between 0 and 180 degrees in an interval of 30 degrees).

The heat transfer coefficient at each power input was then calculated as follows:

$$h = Q/[A(T_{avg} - T_{sat})] \quad (2)$$

where A is the heated area of the tube which contacted with liquid

$$A = N \times \pi \times \{W \times d_1 + (P - W) \times d_2 + 0.5(d_1 \times d_1 - d_2 \times d_2)/\sin\theta + 2 \times d_2 \times H \times \cot\theta + (17.5 - 0.5W) \times d_2\} \quad (3)$$

where N was number of rib elements.

UNCERTAINTY ANALYSIS

An uncertainty analysis was made to consider the errors caused by the interpolation procedure of the measuring instruments. The uncertainty is due to calibration and fluctuation in the thermocouple reading during boiling. The values of the six wall temperatures were recorded and compared to examine variations caused either by nonuniformities in the cartridge heater or by the test tube soldering and assembly procedure. It was found that the maximum variation of the six measured wall temperatures was 0.4°C at maximum heat flux (≈ 80 kW m^{-2}) and 0.2°C at the minimum heat flux (≈ 50 W m^{-2}). As a percentage of the corresponding wall superheat ($T_w - T_{sat}$), the above value corresponds to 13.4%. The variation in wall superheat was ± 0.2°C at high heat flux and ± 0.1°C at low flux. The corresponding uncertainty in the measured heat flux was estimated to be ± 1.0%.

The two liquid pool thermocouple agreed within 0.1°C. The saturation temperature at the measured pressure agreed within 0.1°C. Based on these uncer-

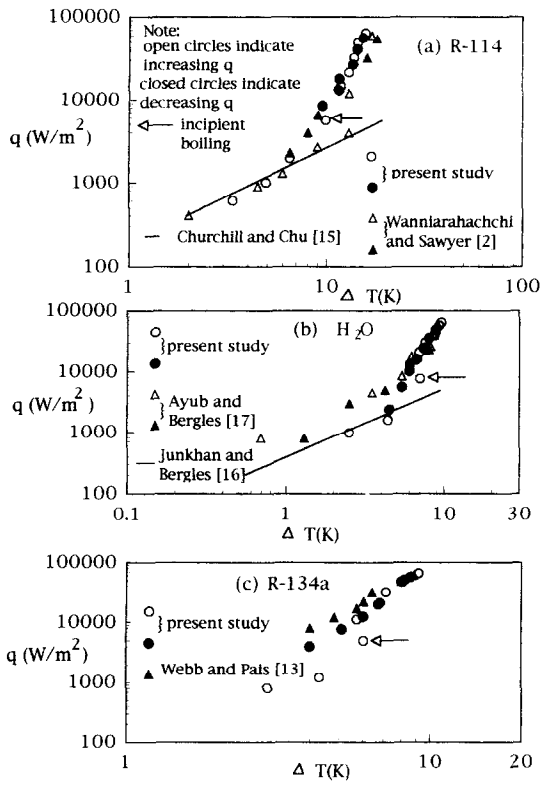

FIG. 3. Smooth tube data for (a) R-114, (b) distilled water, (c) R-134a.

taintics. it gives the uncertainty of wall heat transfer coefficient of about $\pm 9.5\%$.

RESULT AND DISCUSSION

Data for a smooth tube with three different refrigerants as shown in Fig. 3 are used as a reference for the enhancement provided by the other four tubes. Moreover, comparisons were made with those of previous investigators. The incipient boiling condition is indicated by a change in slope when heat flux is plotted vs ΔT since the heat transfer mechanism changes from single-phase convection to two-phase convection with the activation, growth, and departure of vapor bubbles during increasing heat flux (q) runs. A line representing the correlation developed by Churchill and Chu [15] for R-114 and Junkhan and Bergles [16] for distilled water for natural convection from a horizontal cylinder is also shown. It is apparent that the present data are in good agreement with these correlations, showing the reliability of the apparatus and instrumentation used. The smooth tube R-114, distilled water and R-134a tests shown in Fig. 3 were very much expected. The boiling curve for partial and developed boiling was essentially the same for both increasing and decreasing heat fluxes, regardless of rate of heat flux change. Taking careful examination, it is found that a larger incipient boiling superheat is required for R-114 (≈ 10 K) following by distilled water ($\approx$ 6 K) and R-134a ($\approx$ 5 K) and in each

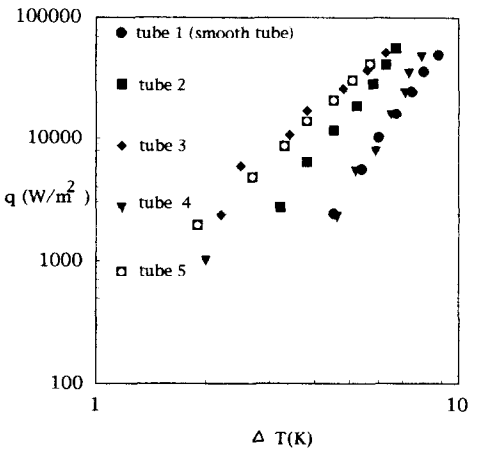

FIG. 4. Boiling data for distilled water for smooth tube/roughened tubes (decreasing heat flux mode).

case a hysteresis pattern is noted. The present boiling curves for three refrigerants are characterized by small-scale boiling curve hysteresis in Fig. 3. Figure 3 also provides a comparison between data obtained during this investigation and data obtained by Wanniarahachchi *et al.* [2] for R-114 as well as by Ayub and Bergles [17] for distilled water and by Webb and Pais [13] for R-134a, respectively. In general, the agreement between the corresponding two investigations for Figs. 3(a)–(c) is excellent. Figure 3 also indicates that there is less temperature overshoot with R-134a and distilled water, dur to the less extensive deactivation of the potential nucleation sites by flooding with liquid. Figure 4 compares the results of roughened tubes under study to the plain (smooth) tube for distilled water during decreasing heat flux. In the fully developed boiling region, it is evident that the best heat performance is shown by Tubes No. 3 and No. 5 followed by Tubes No. 2 and No. 4.

It is interesting that Tube No. 4 seems to have the same performance as that of the smooth tube. Figure 5 repeats the data in Fig. 4 as a variation of the boiling heat transfer coefficient for the nucleate boiling region as a function of the heat flux. In general, the heat

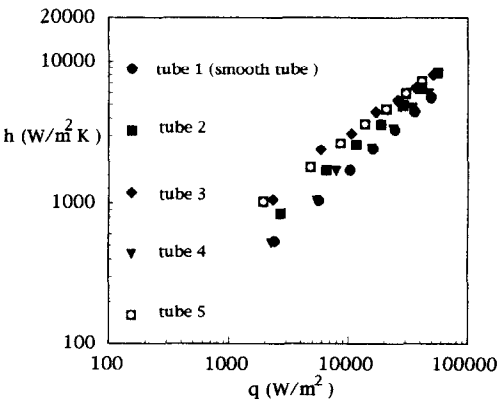

FIG. 5. Heat transfer coefficient vs heat flux for distilled water for smooth/roughened tubes.

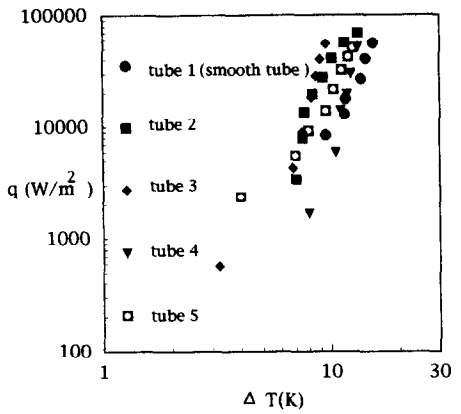

FIG. 6. Boiling data for R-114 for smooth/roughened tubes (decreasing heat flux mode).

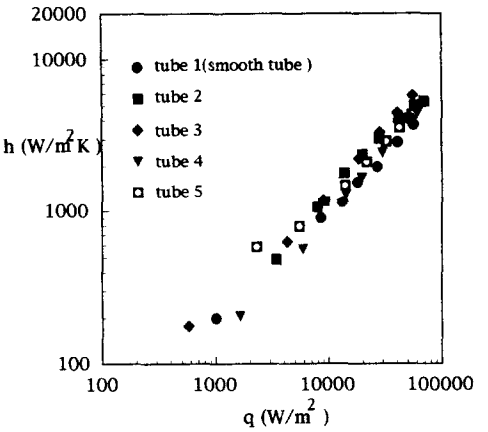

FIG. 7. Heat transfer coefficient vs heat flux for R-114 for smooth/roughened tubes.

transfer coefficient increases as the heat flux is increased. For comparison purpose, the data for the smooth tube are also shown on this figure. It can be seen that Tubes No. 3 and 5 result in a boiling enhancement compared to the corresponding smooth tube data at a specified heat flux (say, 50 kW m^{-2}) of about 1.45. However, for Tube No. 4 the enhancement decreases to about 1.1. Furthermore, the enhancement decreases as the heat flux increases for all the roughened tubes studied herein. This is because with heat flux increase the enhancement deteriorates. At a lower heat flux (say, 2 kW m^{-2}), the heat transfer coefficients with Tubes No. 3 and 5 are about two times the plain tube value. This enhancement factor tapers off to a factor slightly above 1.2 as the heat flux is increased to 80 kW m^{-2}. The other two roughened tubes have the same trend and differ in magnitude for enhancement factor. This is perhaps because, at high heat fluxes, the large tunnels created within the present roughened geometry give it the characteristic of a plain tube with fins, rather than a surface with numerous active sites. However, at low heat fluxes, because of the large spacing between the tunnels, it is speculated that separation of the vapor column occurs. As a result, neighboring vapor columns do not coalesce as readily. This gives a higher heat transfer coefficient. Figure 6 compares the results of each roughened tube to the smooth tube for R-114. In every case, higher measured superheats prior to bubble nucleation were found when compared with those for distilled water shown in Fig. 4. This most likely occurs because of the high wettability of R-114 on roughened surface, the large cavities are flooded with liquid and higher superheats are needed to nucleate smaller cavities. Note that, in comparing the four roughened surfaces, the incipient point occurs at the lowest heat flux and superheat for Tube No. 3. The Tube No. 4 with rib angle of 45° requires the largest superheat due to the ease with which the R-114 can flood the large tunnels between adjacent ribs. Each of the enhanced surfaces requires a lower superheat than the plain (smooth) tube. Figure 7 shows data of Fig. 6, once again expressed as the variation of heat transfer coefficient as a function of the heat flux together with the data for smooth tube. As can be seen, the roughened tube shows a little enhancement (about 1.2) for the entire range of heat flux considered. The influence of heat flux on heat transfer coefficient is significant when R-114 was used as a refrigerant. Of all the roughened surfaces tested in these three different refrigerants, Tube No. 3 consistently experienced the most rapid activation. The rib angle for Tube No. 3 is 60°. This is perhaps because Tube No. 3 (rib angle 60°) provides more regularly spaced re-entrant cavities than those of the remainder of the roughened surfaces (rib angles of 30, 45 and 90°) and greatly enhanced nucleation properties. Exact reasons for this are not understood at this stage. Further study may include this aspect. Figure 8 compares the results of each roughened tube to the smooth tube for R-134a. In every case, higher measured superheats prior to bubble nucleation were found again with those for distilled water shown in Fig. 4. However, these values are a little bit lower than the corresponding superheats required for R-114 shown in Fig. 6. This strongly suggests that, in general, the degree of superheat required to activate the roughened surface is less than the smooth (plain) tube, and

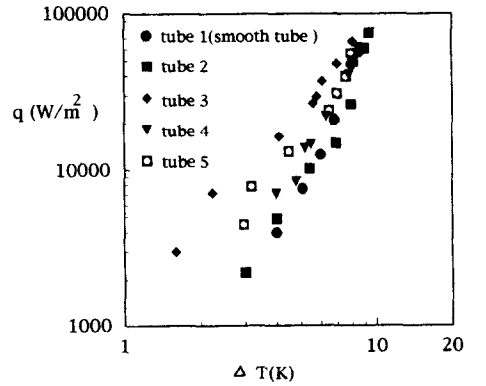

FIG. 8. Boiling data for R-134a for smooth/roughened tubes (decreasing heat flux mode).

is sensitive to both working medium and rib angles. It is found that less superheat is required for distilled water, followed by R-134a and R-114.

Figure 9 shows data of Fig. 8 again, expressing the variation of heat transfer coefficient as a function of the heat flux. Once again, the heat transfer coefficient increases as the heat flux increases. Moreover, the slope seems lower than that in R-114. The enhancement due to roughened tubes is modest compared to Figs. 5 and 7 for distilled water and R-114. In general, comparing Figs. 5, 7 and 9, one may find that the enhancement factor compared to the plain tube at a specific heat flux for four rib angles studied was clearly noted in Fig. 5 for distilled water but less noted in Fig. 9 for R-134a. This is perhaps related to the moderate wetting ability of the distilled water compared to R-134a. In addition, examination of all the data sets shows that the slope of the h vs q curve is not exactly equal for the various refrigerants. This is much more noticeable for the rib-roughened tube than for the plain tube (not shown). This finding coincided with that reported by Webb and Pais [13].

The effect of rib angle upon boiling inception can be examined from the well-known nucleation parameter [18] shown in the following equation for the critical superheat required to nucleate from a vapor-filled cavity. It is worthwhile to note that, with the properties listed in Table 2, the ratio of the parameter for R-114 to distilled water is 1.21. Due to lacking a value of surface tension, M is not available for R-134a.

$$M = \frac{\sigma_l T_{sat}}{\rho_v h_{fg}}. \quad (4)$$

Upon comparing the incipient boiling superheats plotted in Figs. 4, 6 and 8, one can find the following superheat ratios for each of the test tubes for different rib angles:

Tube no. (rib angle)	ΔT(R-114)/ $\Delta T(H_2O)$	ΔT(R-134a)/ $\Delta T(H_2O)$
1 (smooth)	1.42	0.91
2 (90°)	1.23	1.14
3 (60°)	1.60	1.71
4 (45°)	1.38	1.07
5 (30°)	1.15	1.44

These experimentally obtained ratios are in good agreement with the theoretical ratio of 1.21 previously mentioned, implying that the nucleation parameter defined in equation (4) may be a reasonable index of incipient boiling superheats from the roughened surfaces. It is also of interest to mention that, in comparing Figs. 4, 6 and 8, the superheat required at boiling incipience is smallest for Tube No. 3, followed by Tube No. 5, Tube No. 2 and Tube No. 4.

Table 3 documents the present enhancement performance ratios for the present roughened surface geometry considered for three different refrigerants. It is clearly noted that distilled water provides the best heat transfer performance, followed by R-114 and R-134a as also evidenced by Figs. 5, 7 and 9. For a given refrigerant, it is found that Tube No. 3 with rib angle of 60° has the highest enhancement, followed by Tube No. 5 (rib angle 30°), Tube No. 2 (rib angle 90°) and Tube No. 4 (rib angle 45°) which is also seen in Figs. 5, 7 and 9. There seems no clear trend between the heat transfer performance and the rib angle. Again this needs further study for an explanation.

Finally, the present rib-roughened Tube No. 3 results were compared with those from Webb and Pais [13] for R-134a with GEWA SE, K26 and TX19 surfaces as shown in Fig. 10. It is apparent that the trend for the influences of the heat flux on heat transfer coefficient is almost the same (i.e. has the same slope ≈ 0.7) but the magnitude is different. The enhanced surfaces considered in Webb and Pais [13] are higher than the present Tube No. 3. But, nevertheless, the present rib-roughened geometry still improves heat transfer a bit.

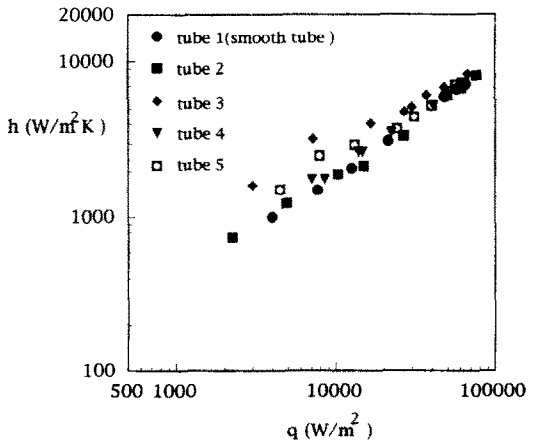

FIG. 9. Heat transfer coefficient vs heat flux for R-134a for smooth/roughened tubes.

CONCLUSION

The study of pool boiling from rib-roughened tubes and a plain tube of three different refrigerants has established that, in addition to boiling curve data and hysteresis identification, heat transfer enhancement is to be expected with a moderately wetting liquid such as water and highly wetting liquids such as R-114. These results lead to the following conclusion.

1. The heat transfer for roughened tubes is consistently higher than that in the plain tube for the three refrigerants considered herein. For distilled water, the roughened surfaces show a 1.05–1.93 increase in heat transfer coefficient when compared to the plain tube. For a definite rib geometry, rib angle 60° exhibits the highest heat transfer performance in these refrigerants. However, for R-134a, the enhance-

Table 3. Enhancement performance ratio for the surface geometry under study for three refrigerants

Fluid	q (W m^{-2})	Tube No. 1		Tube No. 2		Tube No. 3		Tube No. 4		Tube No. 5	
		h (W m^{-2} K^{-1})	Enhancement performance ratio†	h (W m^{-2} K^{-1})	Enhancement performance ratio	h (W m^{-2} K^{-1})	Enhancement performance ratio	h (W m^{-2} K^{-1})	Enhancement performance ratio	h (W m^{-2} K^{-1})	Enhancement performance ratio
Distilled water	5000	1104	1.00	1392	1.39	1942	1.93	993	0.99	1854	1.85
	10 000	1730	1.00	2334	1.35	2707	1.56	1706	0.99	2907	1.68
	20 000	2872	1.00	3766	1.31	4700	1.64	3008	1.05	4459	1.55
	30 000	3887	1.00	5107	1.31	5745	1.48	4195	1.08	5728	1.50
	40 000	4747	1.00	6384	1.34	6975	1.47	5289	1.11	7039	1.48
	50 000	5601	1.00	7593	1.36	8074	1.44	6179	1.10	8187	1.46
R-114	5000	544	1.00	660	1.21	687	1.26	481	0.88	624	1.15
	10 000	928	1.00	1362	1.47	1296	1.40	913	0.98	1126	1.21
	20 000	1591	1.00	2393	1.50	2402	1.50	1675	1.05	1959	1.23
	30 000	2167	1.00	3185	1.47	3415	1.58	2422	1.18	2722	1.26
	40 000	2797	1.00	3979	1.42	4401	1.57	3179	1.14	3367	1.20
	50 000	3377	1.00	4681	1.39	5344	1.58	3821	1.13	4020	1.19
R-134a	5000	992	1.00	1242	1.25	2373	2.30	1020	1.03	1655	1.65
	10 000	1783	1.00	1699	0.95‡	3446	1.93	1948	1.09	2668	1.49
	20 000	2974	1.00	2682	0.90	4267	1.42	3293	1.11	3413	1.15
	30 000	4061	1.00	3773	0.93	5183	1.28	4235	1.04	4323	1.06
	40 000	5137	1.00	5572	1.08	6279	1.22	5154	1.01	5348	1.02
	50 000	6137	1.00	6136	1.00	6992	1.14	6120	1.00	6349	1.03

† Enhancement performance ratio = $h_{\text{Tube No. } i}/h_{\text{Tube No. 1}}$, $i = 2, 3, 4, 5$.

‡ Underlining indicates that the enhancement performance is less than that of the smooth tube.

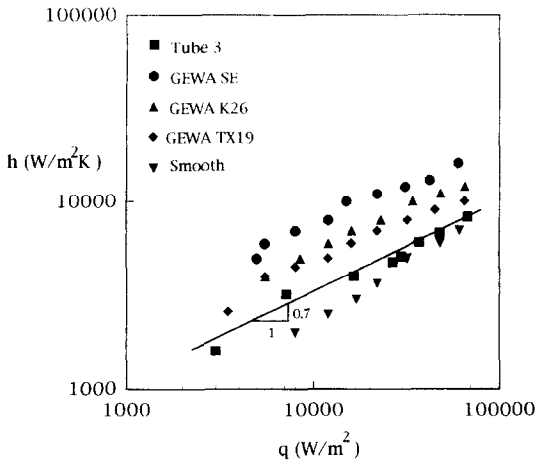

FIG. 10. Comparison of Tube No. 3 with GEWA SE, K26, TX19 and smooth tube (from Webb and Pais [13]) for R-134a.

ment from roughened surfaces seems insignificant when compared to a smooth tube.

2. Roughened ribs give the higher heat transfer performance over a range of heat fluxes, Tubes No. 3 and 5 (rib angle 60° and 30°) consistently perform well in three different refrigerants.

3. Generally speaking, the degree of superheat required to activate the enhancement surfaces is less than the plain tube, and is sensitive to both working fluid (i.e. the refrigerants) and rib angles. The superheats for the plain tube required for R-114 are approximately twice as large as those required for distilled water, which is in agreement with existing theory. Consequently, the temperature overshoot problem and resulting nucleate boiling hysteresis pattern is less severe with distilled water than with R-114.

4. The influences of heat flux on enhanced heat transfer coefficients are almost the same as those reported by previous investigators which indicates they have the same slope of 0.7.

5. Enhancement performance ratios defined in Table 3, for the present roughened surface geometry considered for three different refrigerants, were calculated, and it is found that distilled water provides the best heat transfer performance, followed by R-114 and R-134a.

Acknowledgement—This work was supported by a research grant (NSC 82-0401-E110-128) from the National Science Council, Taiwan, R.O.C. Revision assistance of this paper from one of the leading author's Ph.D. students, Mr. Mao-Yu Wen, is greatly appreciated.

REFERENCES

1. R. L. Webb, The evolution of enhanced surface geometries for nucleate boiling, *Heat Transfer Engng* **2**(3-4), 46–69 (1981).
2. A. S. Wanniarahachchi, L. M. Sawyer and P. J. Marto, Effect of oil on pool boiling performance of R-114 from enhanced surfaces, *ASME–JSME Thermal Engineering Joint Conference*, Vol. 1, pp. 531–537 (1987).
3. A. C. Grant, Porous Metallic Layer Formation, U.S. Patent 3, 821, 018 (1974).
4. J. Fujikake, Heat Transfer Tube for Use in Boiling Type Heat Exchangers and Method of Producing the Same, U.S. Patent 4, 216, 826 (1980).
5. K. Fujie, W. Nakayama, H. Kuwahara and K. Kakizaki, Heat Transfer Wall for Boiling Liquids, U.S. Patent 4, 060, 125 (1977).
6. M. Saier, H. W. Kastner and R. Klochkler, Y and T-Finned Tubes and Methods and Apparatus for Their Making, U.S. Patent 4, 179, 991 (1979).
7. Wieland-Produktinformation, GEWA-T Tubes: High Performance Tubes for Flooded Evaporators, Wieland-Werke AG, Ulm, West Germany.
8. P. J. Marto and V. J. Lepere, Pool boiling heat transfer from enhanced surface to dielectric fluids, *Adv. Enhanced Heat Transfer* ASME HTD—Vol. 18, 93–102 (1981).
9. E. Hahne, Q. R. Chen and R. Windisch, Pool boiling heat transfer on finned tubes—an experimental and theoretical study, *Int. J. Heat Mass Transfer* **34**, 2071–2079 (1991).
10. Z. H. Ayub and A. E. Bergles, Nucleate pool boiling curve hysteresis for GEWA-T surfaces in saturated R-113, *ASME Proceedings of the 1988 National Heat Transfer Conference*, Vol. 2, pp. 515–522 (1988).
11. D. B. R. Kenning, Wall temperature patterns in nucleate boiling, *Int. J. Heat Mass Transfer* **35**, 73–86 (1992).
12. M. C. Chyu and J. Fei, Enhanced nucleate boiling in an angular geometry found in structured surface, *Int. J. Heat Mass Transfer* **34**, 437–447 (1991).
13. R. L. Webb and C. Pais, Nucleate pool boiling data for five refrigerants on plain, integral-fin and enhanced tube geometries, *Int. J. Heat Mass Transfer* **35**, 1893–1904 (1992).
14. E. Hahne and J. Muller, Boiling on a finned tube and a finned tube bundle, *Int. J. Heat Mass Transfer* **26**, 849–859 (1983).
15. S. W. Churchill and H. H. S. Chu, Correlating equations for laminar and turbulent free convection from a horizontal cylinder, *Int. J. Heat Mass Transfer* **13**, 1049–1053 (1975).
16. C. H. Junkhan and A. E. Bergles, Heat transfer laboratory data acquisition system, Heat Transfer Laboratory Report HTL-12, ISU-ERI-Ames-77178, Iowa State University, Ames, Iowa (1976).
17. Z. H. Ayub and A. E. Bergles, Pool boiling from GEWA surfaces in water and R-113, *ASME Winter Annual Meeting*, Miami, FL, November (1985).
18. A. E. Bergles and W. M. Rohsenow, The determination of forced convection surface-boiling heat transfer, *ASME J. Heat Transfer* **86**, 365–372 (1964).